Dynamical evidence of critical fields in Josephson junctions

M. Cirillo
Dipartimento di Fisica, Università di Roma ''Tor Vergata,'' I-00133 Roma, Italy

T. Doderer and S. G. Lachenmann*
Universität Tübingen, Lehrstuhl Experimentalphysik II, D-72076 Tübingen, Germany

F. Santucci
Dipartimento di Energia Elettrica, Università di L'Aquila, I-67040 L'Aquila, Italy

N. Grønbech-Jensen
Theoretical Division, Los Alamos National Laboratory, Los Alamos, New Mexico 87545
and Department of Physics, University of California, Los Angeles, California 90024
(Received 26 March 1997; revised manuscript received 26 June 1997)

We study the dynamical stability of phase configurations generated by an external magnetic field in long Josephson junctions. Depending on the value of the field, the penetration of the vortex lines through the boundary of the junctions gives rise to different dynamical regimes whose nature is characterized by measurements of Fiske singularities in the current-voltage characteristics of the junctions. The magnetic-field dependence of the height of these singularities is compared with numerical simulations of the sine-Gordon equation and low-temperature scanning electron microscopy of the junctions is performed in order to validate the dynamical patterns. For all the junctions that we have investigated, given their maximum pair current density j_c and the Josephson penetration depth λ_j, we find that the external magnetic field that equals the critical value $H_0=2\lambda_j j_c$, responsible for the trapping of a single static flux-quantum in the junction, plays a dominant role in establishing dynamical phase configurations. Both simulations and low-temperature scanning electron microscopy show complete analogy between the dynamical patterns of long and small-area junctions when H_0 is exceeded. [S0163-1829(97)02542-3]

I. INTRODUCTION

Long Josephson junctions have been investigated intensively due to the importance of magnetic-flux quanta (physical manifestation of solitons) for solid-state physics and applied mathematics.[1] Based on perturbation techniques for fluxon dynamics, numerous experimental features of long junctions have been successfully characterized—even for very intriguing cases in which the junction is driven by time-dependent perturbations.[2] Also, coupling of several junctions through their boundaries[3] or mutual coupling in adjacent junction structures[4] has been investigated.

The studies can be divided into two categories. In the first category we find sine-Gordon solitons traveling through a medium determined by the value of the bias current (which may also be time dependent) and a small magnetic field confined to the boundaries of the junction. In this case one can extract detailed information about the physics of the problem from the McLaughlin and Scott theory[5] as the aim of that theory was to investigate the steady-state motion of fluxons (and other solutions of the sine-Gordon equation) under small perturbations. In the second category we find arrays of vortices distributed along one[6] (or two[7,8]) dimensions of the junctions driven by dc (Ref. 6) and (or) rf (Ref. 9) currents. The physics of this category cannot be treated by the McLaughlin-Scott perturbation theory for solitons as the perturbations (bias current and magnetic field) are no longer small compared to the sine-Gordon terms. Thus, numerical simulations are usually employed to fit experimental data, but models and conjectures characteristics of small-area Josephson junctions often describe basic experimental features.

The internal dynamics of ''flux-flow'' oscillators[6,7] (successfully employed in integrated receivers for radio astronomy) falls in the second category mentioned above since the one-dimensional array of vortices can only be generated by a ''strong'' magnetic field.

The aim of the present paper is to establish quantitatively, and in terms of externally applied magnetic fields, the limiting regimes for which long Josephson-junction dynamics can be classified in one of the two above categories. Understanding the dynamical regimes of a long Josephson junction can be strictly related to their thermal (and thermodynamic) properties.[10] In the present work an attempt is made to establish a link between magnetic field penetration, phase patterns of the junction, and thermodynamic properties of long Josephson junctions.

The paper is structured as follows: in the next section we review the phenomenology of current singularities in the current-voltage characteristics of long Josephson junctions and present the experimental results that we have obtained on several junctions of different geometries fabricated by Nb-lead alloy technology.[11] In Sec. III we show results of low-temperature scanning electron microscope (LTSEM) investigation of junction dynamics when the biasing conditions

are as described in Sec. II. In Sec. IV we present the results of numerical simulations of a long Josephson-junction model and compare the numerical predictions with the experimental findings. In Sec. V we conclude the paper. In the Appendix we shortly review the notations and normalizations of critical magnetic fields in long Josephson junctions.

II. FISKE MODES PHENOMENOLOGY

Before discussing the behavior of the Fiske steps when applying an external magnetic field, we review the internal dynamics of long one-dimensional Josephson junctions in terms of singularities observed in their current-voltage characteristics. The internal dynamics of large-area Josephson junctions is very complicated and we therefore restrict our attention to one-dimensional junctions, where the relevant length is measured relative to the Josephson penetration depth $\lambda_j=\sqrt{\Phi_0/2\pi\mu_0 d j_c}$, $\Phi_0=2.07\times10^{-15}$ Wb being the magnetic-flux quantum, $d=\lambda_1+\lambda_2+t=250$ nm (Ref. 11) is the magnetic thickness of the junction, and j_c is the maximum Josephson current density in the junctions.

In the absence of external magnetic fields, long one-dimensional junctions of overlap and inline geometries[14] exhibit singularities in the current-voltage characteristic called zero-field steps[1] that appear near asymptotic voltages $V_N=N\overline{c}\Phi_0/L$, where $N=1,2\ldots$ is the number of flux quanta participating in the oscillations, L is the physical length of a junction and $\overline{c}$ is the characteristic velocity (the linear electromagnetic wave propagation velocity in the oxide barrier). The difference between the two geometries is that the overlap geometry directs the bias current perpendicular to the direction of propagation of the fluxons while, the two directions are parallel for the in-line geometry. Although a complete theory for these singularities does not exist (the current height of the steps, for example, has not been understood yet), numerical simulations, perturbation theory approaches, and analytical solutions give sufficient information about the internal dynamics of the junctions. Applying a magnetic field to the junctions perpendicular to the direction of propagation of the fluxons, the zero-field steps exist only for a limited magnetic field interval which depends on the length of the specific junction under investigation.[12,13] Further increase of the magnetic field leads to the appearance of current singularities (Fiske steps) at asymptotic voltages $V_k=k\overline{c}\Phi_0/2L$ where $k=1,2\ldots$ is the step order number. We note that for every V_k corresponding to an even integer k, there is a zero-field step V_N ($N=k/2$). However, this can be viewed as a coincidence since, as we shall see, the physical phenomena generating the two families of singularities are different. The aim of the present work is to quantify the critical field above which the Fiske steps appear and to understand the dynamics in the junction.

In Fig. 1 we show a typical magnetic-field modulation pattern of the Josephson current and of the first three Fiske singularities of a junction having a normalized length $l=L/\lambda_j=7.5$. This is a junction of overlap geometry in the sense that the extended dimension is perpendicular to the direction of the bias current, but, as the junction is obtained through a window in the SiO insulating layer, small asymmetries in the biasing conditions at the boundary can be expected. For this reason the Josephson current does therefore not have its maximum for precisely zero applied external field. The most relevant difference between zero-field steps and Fiske steps is that the zero-field steps have a current amplitude which decreases monotonically with the step order number, while the current height of the Fiske steps modulates with the order number for any value of the external magnetic field.

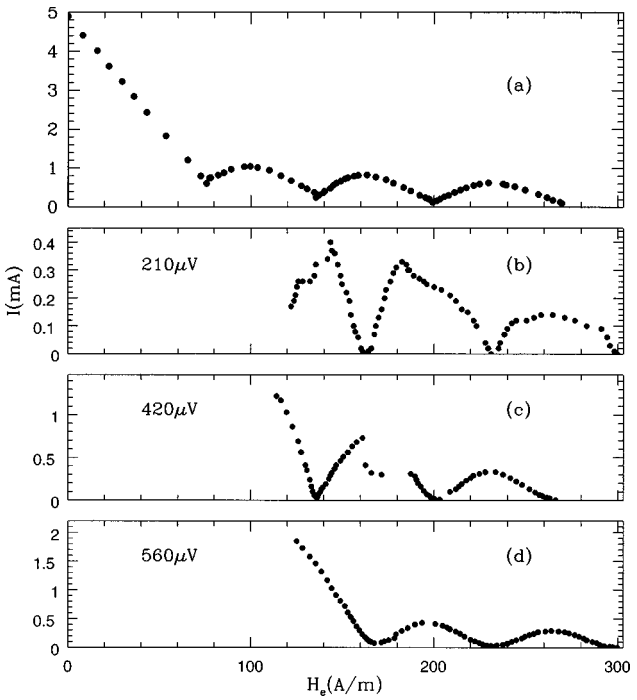

FIG. 1. Modulation patterns of a one-dimensional overlap junction of length $7.5\lambda_j$. (a) Josephson current; (b), (c), and (d) are first, second, and third Fiske steps, respectively.

We see that the value of the field for which the stable modulations of the Fiske modes begins is 110 A/m, a little above the value where the Josephson current attains its first zero (around 80 A/m). We note that, below this value of the field, it is sometimes possible to observe current steps at the voltage values corresponding to the Fiske step voltages, but these solutions are very unstable and characterizing these states is very difficult.

In Fig. 2 we show the equivalent of Fig. 1 for an in-line junction having a normalized length $l=7$. This junction was fabricated over a superconducting ground plane and the observed asymmetry of the central lobe of the modulation pattern is therefore expected.[14] We can see that the behavior of the modulations is similar to the overlap junction: the stable modulations of the field begin when the critical field $H_e=80$ A/m is exceeded (just above the value for which the Josephson current has its first minimum). The role of this field value for the in-line junctions was well pointed by Owen and Scalapino[15] for the static properties. This field corresponds to the maximum value for which the Meissner solution is possible. One static flux quantum is trapped in the junction (in the limit $l\gg1$) for this applied magnetic-field value.

The data of Figs. 1 and 2 show that the modulations of the current singularities that begin right above the critical field have the same characteristics as the modulations of the Fiske steps in small junctions. Also, there is another typical feature

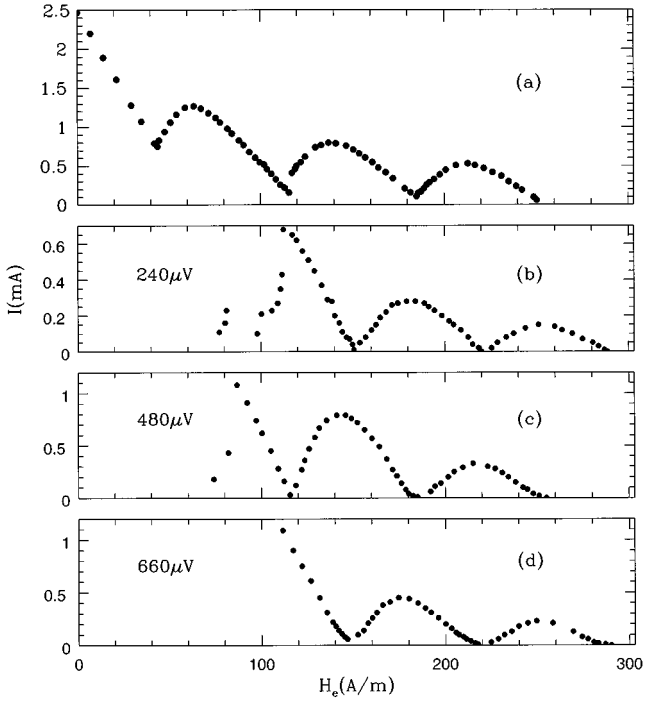

FIG. 2. Modulation patterns of an inline junction of length $7\lambda_j$. (a) Josephson current; (b), (c), and (d), respectively, are first, second, and third Fiske steps.

of Kulik's model[19] which is represented in our data. We find that the modulations of the first two modes of Fig. 1 present somewhat irregular points, while the third is more stable. In contrast to this we find in Fig. 2 that all three modulations—once started—present very regular points. The reason for this difference might be the fact that, when the voltage of the steps is below the plasma voltage of the junctions, the cavity mode excitations interact with the plasmons and the theoretical model is no longer valid. The plasma voltage (the voltage corresponding to the plasma frequency on the basis of the Josephson ac equation) of the junctions of Figs. 1 and 2 is 300 μV and the trend of the data is therefore more regular above this value. In longer junctions with the same current density and plasma voltage we have seen that the modulations with the applied magnetic field are less regular even when the critical field ($\sim$80 A/m) is exceeded. In the next section we find that the dynamical patterns of the phase inside long junctions are of the same type as in small junctions.

III. OSCILLATIONS ANALYSIS—LTSEM IMAGING

We have performed a LTSEM investigation of two in-line junctions located on the same chip and having physical lengths of 60 and 50 μm, respectively. On the 50-μm-long junction we concentrated our attention on the analysis of the oscillations when current biased on the first Fiske step, while on the 60-μm-long junction we investigated several steps.

In Fig. 3 we see the LTSEM voltage images[17,18] for the second, third, and fourth Fiske steps of the 60-μm-long inline junction with normalized length $l=2.5$ taken for field values of 116, 180, and 220 A/m, respectively. All the data in this section were taken for magnetic-field values allowing for stability of the steps and generating amplitude modulations as described in the previous section. The field generating the first zero of the Josephson current was 160 A/m in both of the cases we investigated.

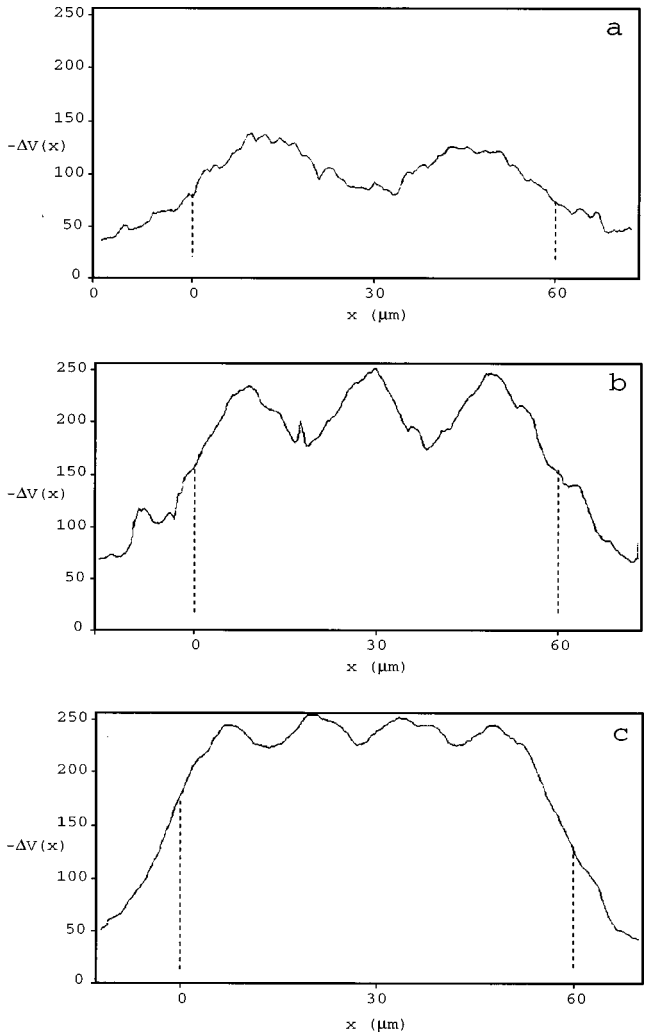

FIG. 3. LTSEM voltage (in arbitrary units) response profiles for a 60 μm long in-line junction (2.5 in normalized units). In (a), (b), and (c) the junction was dc biased, respectively on the second, third, and fourth Fiske steps. We see that all the excitations are single-mode oscillations. The edges of the junction are indicated by dashed lines.

Details of the LTSEM technique of imaging internal dynamics of Josephson junctions have been well described in a number of publications. In particular, the imaging techniques and the interpretations of dynamical patterns related to Fiske steps have been described in Ref. 18. In order to obtain the images shown in Figs. 3 and 4, we current biased the junction on the Fiske step and recorded the electron-beam-induced voltage change $\Delta V(x)$ as a function of the beam's coordinate x. As shown in Ref. 18, $-\Delta V(x)$ represents the spatial distribution of the square of the magnetic field related to the cavity mode in the time average.

Comparing these pictures with the patterns[18] obtained on other samples for Fiske steps in Josephson junctions we can conclude that we are observing single-mode (Kulik-like[16,19]) oscillations. More multimodelike excitations (not shown in the figure) are observed on the first step at low fields. Figure 4 exemplifies that increasing the external field makes the dynamics more single mode in nature. These two pictures

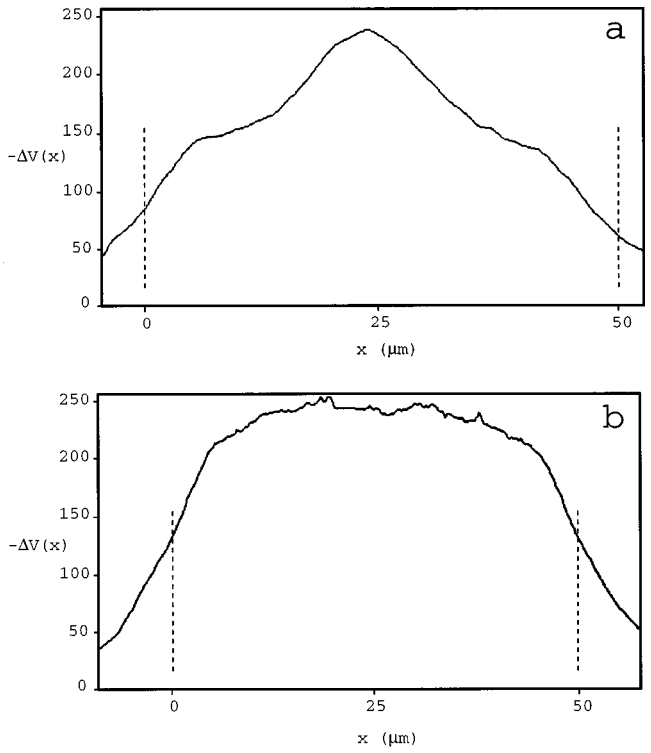

FIG. 4. LTSEM voltage response profile of the first Fiske step of a 50-μm-long in-line junction obtained for increasing values of the external magnetic field. In (a) and (b) the field is 170 and 900 A/m, respectively. As in Fig. 3, the edges of the junction are indicated by dashed lines.

were taken from the systematic analysis of the first Fiske step of the 50 μm-long junction for field values of 170 and 900 A/m, respectively.

Figures 3 and 4 indicate the reason for why modulations like the ones of the steps shown in Fig. 1 can be well fitted by the theory of Kulik.[20] This theory quantitatively predicts the modulations of the maximum currents of the Fiske steps on the basis of a single-mode excitation model of the Josephson transmission line provided the frequency of the modes is larger than the plasma frequency of a junction. The irregular modulations of the first two steps in Fig. 1 are likely connected to ''multimode'' behavior of the first step of the family shown in Fig. 3. The Josephson plasma frequency $\omega_j/2\pi=1/2\pi\sqrt{2\pi j_c/\Phi_0 C}$ of the samples of Figs. 3 and 4 is 67 GHz and its equivalent voltage is 140 μV. In the definition of ω_j the parameter $C=14$ μF/cm^2 is the capacitance/unit area for our junctions. Thus, the first step of the junction is close to the plasma voltage, but tuning the voltage by the magnetic field[21] we drive it above the plasma frequency resulting in stable single-mode oscillations.

In previous[18] LTSEM investigations of the Fiske steps it was evident that the nature of the oscillations was single mode, but the point that we intend to stress in this paper is that no stable LTSEM scanning can be performed on long junctions for field values below the critical field corresponding to the first zero of the Josephson current. This is an important point when dealing with Fiske modes in long junctions, since the theory by Kulik can explain the steps only when the length of the junctions is smaller than the Josephson penetration depth. Our data show that magnetic-field penetration into the junction can generate real single-mode oscillation patterns when the applied field is sufficiently strong. This feature was successfully used when analyzing phase locking of Fiske and flux-flow steps in long junctions[22] and coupled long junctions.[23]

The results presented in this section have shown evidence for the notion that the oscillations associated with stable Fiske modes in long junctions are cavity modes. We wish to quantitatively estimate the threshold field for which the Fiske steps appear in long junctions. After the initial numerical simulations based on a soliton model for these current singularities,[24–26] and later qualitative conjectures,[12] a systematic analysis is very helpful in order to establish the ranges of stability/existence and, in terms of these, the resulting nature of the oscillations. In the next section we report on the investigation, performed over a wide range of junction lengths, of the onset of stable Fiske modes in long junctions.

IV. NUMERICAL SIMULATIONS AND DISCUSSION

We have made a systematic investigation of the system

$$\phi_{tt}-\phi_{xx}+\alpha\phi_t+\sin\,\phi=\gamma, \tag{1}$$

$$\phi_x(t,0)=\phi_x(t,l)=\eta, \tag{2}$$

where $\gamma=I/I_c$ is the bias current normalized to the critical Josephson current, $\alpha=1/\sqrt{\beta_c}$ is a damping parameter related to the McCumber hysteresis parameter β_c,[14] and $\eta=H_e/\lambda_j j_c$ is the normalized magnetic field. Equations (1) and (2) imply that we restrict our interest to junctions with overlap geometry. Time in these equations is normalized to the inverse of ω_j and distance is normalized to λ_j. The system (1)–(2) was discretized and integrated by a second-order central difference algorithm.[16] A damping parameter of $\alpha=0.1$ was used for all our simulations. The magnetic-field dependence of the Fiske steps was taken by recording the current-voltage characteristic of the junction for each value of the normalized field and recording the switching point at the top of the steps. In the current-voltage characteristic every voltage point was obtained after integration of the voltage of the junction for a time corresponding to thousands of periods of mode oscillation.

Figures 5(a) and 5(b) show the Josephson current diffraction pattern and the magnetic-field dependence of the height of the first Fiske step calculated for a junction with a normalized length $l=3$. We see that the stable modulations of the steps begin near the value $\eta=2$, which is also the value where the first lobe of the Josephson current extrapolates to zero. In Figs. 5(c) and 5(d) we see the same patterns for a junction of length $l=8$: also in this case we see that the modulations of the current singularity begin for the same field value as above ($\eta=2$). The steps were not stable below the critical value although coherent oscillations generating voltage points could be recorded very occasionally.

We have seen that the field value for which the stable modulations of the first Fiske modes begin is always $\eta\cong 2$ independently of the junction length l, when this parameter is also larger than two. An example of the dependence of the critical field on the junction length is shown in Fig. 6(a). All the data in Fig. 6 were obtained for $\alpha=0.252$ integrating the system (1)–(2) from flat initial data [$\phi(0,x)=0$,

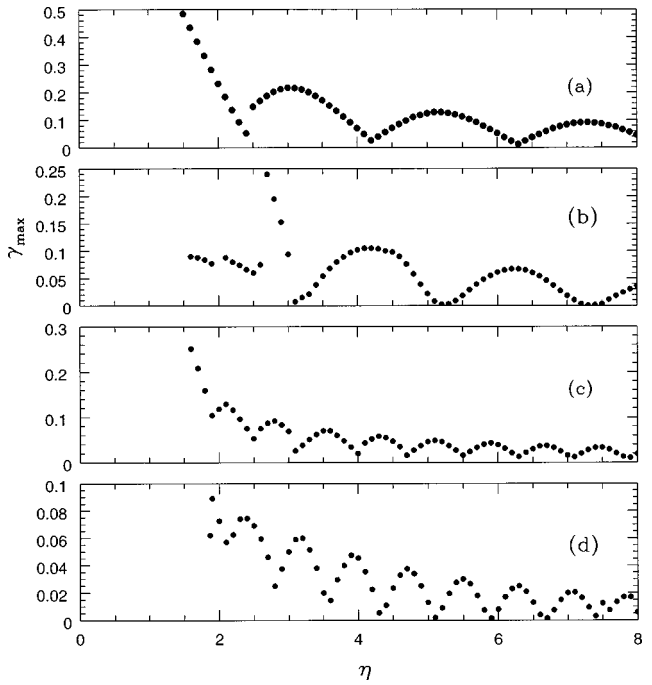

FIG. 5. (a) and (b), respectively: Josephson current diffraction pattern and first Fiske step calculated for an overlap junction having a normalized length $l=3$; (c) and (d), respectively, Josephson current and first Fiske step for a junction having $l=8$. The figure shows the numerical evidence that stable dynamical cavity mode-like oscillations take place above the critical field $\eta=2$ independently of the length of the junction.

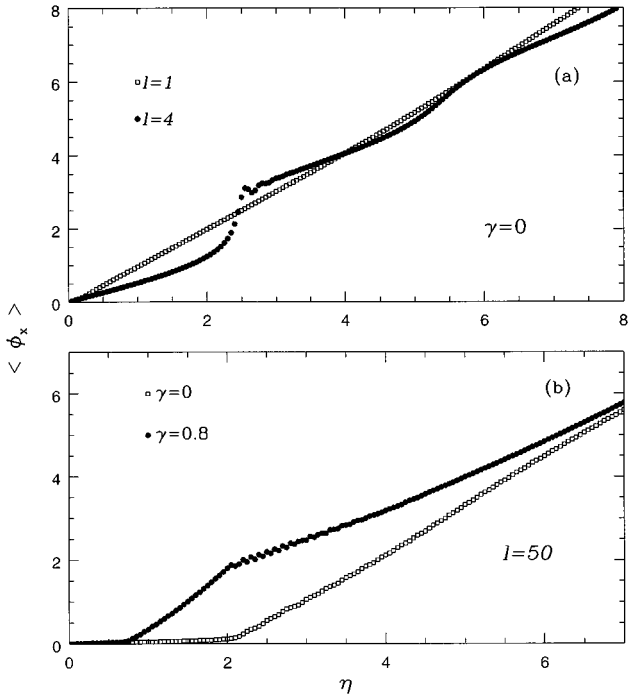

FIG. 6. (a) The onset of the critical field above the critical length of the junction: we plot the spatially averaged value of ϕ_x in the junction as a function of the external magnetic field. The empty squares show the straight line behavior obtained for $l=1$ while, for $l=4$ (full dots) the onset of a discontinuity for $\eta=2$ is evident; (b) same ''magnetization'' curves as in (a) for a junction with length $50\lambda_j$. Above the critical value $\eta=2$ the magnetic field penetrates in the junction, determining the linear increase of the average current, while below this value the field remains confined at the edges of the junction. The empty squares are obtained for zero bias current, while the full dots are obtained for a bias current $\gamma=0.8$

$\phi_t(0, x)=0,\ \gamma=0,\ \eta=0]$ and then observing its dynamical evolution increasing the value of the magnetic field in steps of $\Delta\eta=0.05$. In the figure we show the dependence of $\langle\phi_x\rangle$ (the spatially averaged surface current) upon the external magnetic field. For $l=1$ there is no threshold value for the appearance of the step and the average current depends linearly on the applied field. However, for $l=4$ the discontinuity around $\eta=2$ is already very obvious.

It is natural to picture the physical mechanism leading to the magnetic-field threshold by the numerical experiment described above. In Fig. 6(b) we can see a ''magnetization'' plot obtained for a junction having $l=50$ with an abrupt change of slope taking place for $\eta=2$. Below $\eta=2$ the magnetic field remains confined at the ends and there is no effect inside the junction. It is worth noting that this situation can depend on the dc bias current. We see (open circles) that for $\gamma=0.8$ the ''magnetization'' plot is different since the field penetrates now for $\eta\geqslant 0.8$. Since we have smaller values of the bias current at the bottom of the step, it follows that very stable Fiske modes can be observed only when the system has stability for bias current values close to zero. Therefore, the real threshold for the observation of the stable cavity mode oscillations is $\eta=2$ which corresponds, in SI units, to $H_e=2\lambda_j j_c$. Now we define $H_0=2\lambda_j j_c=\Phi_0/\mu_0\pi\lambda_j d$.

The results of the numerical simulations of the system (1)–(2) reported in Ref. 26 are in good agreement with our analysis. In fact, in Ref. 26 stable soliton mode oscillations were reported for a junction having a normalized length $l=5$, a fixed value of the applied $\eta=0.8$ and a loss parameter $\alpha=0.252$. Due to this high damping parameter, many of the inherent dynamical instabilities present in (realistic) underdamped systems are avoided, and it is therefore possible to stabilize peculiar modes in some regions of the parameter space. However, we do note that the bias current level for which singularities at the same voltages of the Fiske steps could be generated by soliton oscillations were always above $\gamma=0.5$;[26] thus, these oscillations could well justify unstable current singularities in real junctions which is indeed what we observe in the experiments.

A detailed study of the instabilities taking place before the $\eta=2$ threshold was reported in Ref. 25. In this region we have seen that the penetration (respectively, the expulsion) of the field, are favored for high (respectively, low) values of the bias current [see Fig. 6(b)]. The presence of these two tendencies for different bias-current values constitutes a valid background for the onset of chaotic phenomena. Intermittency effects were observed[25] for $\eta=1.25$, normalized length $l=5$, and a loss parameter $\alpha=0.252$ meaning that the conflicting phenomena persist even for a relatively high value of the loss factor. In our simulations, performed for $\alpha=0.1$, we found it very difficult to record voltages below $\eta=2$. Also, our results are not contradicting the original work by Olsen and Samuelsen[24] in which the soliton-oscillation-based model for Fiske steps was proposed. These authors indeed investigated only the range $-2<\eta<2$.

From extensive numerical simulations of long overlap

junctions we found that the first zero of the Josephson current is always at $\eta \cong 2$, independently upon the length as long as $l \geqslant 2$. This result is not surprising considered the results of Owen and Scalapino[20] for in-line junctions and the analysis of Pagano, Ruggero, and Sarnelli[27] for overlap junctions. Stable field penetration in the long junction takes place above the critical field H_0. It is surely remarkable, however, to observe the dynamical features associated with this phenomenon: above H_0, i.e., above $\eta = 2$, the long junction behaves (even temporally) as a small one and all the experimentally observed periodic features of Fiske and ''flux-flow'' steps can be well explained[20] in terms of the early theoretical analyses of the interaction of the ac Josephson effect with cavity modes.[14,16,28]

The simulations show that, for a loss factor $\alpha = 0.1$ and normalized lengths above four the modulations start quite precisely at $\eta = 2$. In real junctions where the loss parameter is lower at least by one order of magnitude it is not surprising that a magnetic field slightly above $H_0$is needed in order to stabilize the oscillations, especially when the frequency of the steps is below the plasma frequency.

For clarity we devote this paragraph to a conjecture (based on dynamical arguments) presented previously[12] concerning the analogy between the long Josephson junction and a type-II superconductor. We have seen above that the reason for generating dynamical instability below the threshold field is not the Josephson background ($\gamma = 0$) in the presence of a field but the additional effect of the dc bias current. Therefore, there is indeed only one critical field above which stable penetration (and stable Fiske steps) take place. This field is H_0 ($\eta = 2$ in normalized units). When $H_e < H_0$, the field penetration is enhanced for high bias-current values and this phenomenon can give rise to dynamical instabilities. However, it can be misleading to explain the phenomena taking place in this interval as behavior of mixed-state type-II superconductors since H_0 is not analogous to the upper critical field.[32] A detailed study of the magnetization effects of long Josephson junctions has recently been reported by Chen and Hernando;[33] their results are consistent with our data in Fig. 6.

V. CONCLUSIONS

In this paper we have identified the dynamical regimes and the parameters generating stable Fiske mode oscillations in long Josephson junctions. These oscillations are generated in long junctions (as well as in small ones) by interaction of the ac Josephson effect with the cavity modes. However, in long junctions, this is possible only when, for junction lengths larger than 2, a critical field is exceeded. We have shown that the (normalized) value of the critical field is 2, (the value which allows complete penetration of one vortex into the junction) independently upon junction geometry (overlap or inline). The nature of the oscillations has been displayed by LTSEM analysis and modulation patterns of the current singularities generated by cavity oscillations. This work relates directly to the interpretation of many experimental situations where Fiske modes are essential, such as, e.g., diagnostic tools for coupled junction systems,[4] discrete Josephson transmission lines,[29] and high T_c Josephson junctions.[30,31] All these examples touch the more general area of spatially distributed oscillations extending more than the characteristic penetration depth. A quantitative clarification of the behavior of Fiske modes in the continuum limit for a single long junction may therefore constitute an important reference point.

ACKNOWLEDGMENTS

The junctions used for the presented experiments were fabricated by M. Cirillo and F. Santucci at the IESS-CNR (Rome). We wish to thank P. Carelli, M. G. Castellano, R. Leoni, and G. Torrioli for allowing us to use the junction fabrication equipment in their laboratory (IESS-CNR, Rome). We also thank G. Verona Rinati for skillful help during the collection of the data that led to Figs. 1 and 2. Parts of this work were conducted under the auspices of the U.S. Department of Energy, supported by funds provided by the University of California for the conduct of discretionary research by Los Alamos National Laboratory; our work took substantial advantage from accessing the computing facilities of the Advanced Computing Laboratory (Los Alamos).

We acknowledge Professor Robert Dana Parmentier whose contributions to the research in the field of long Josephson junctions are invaluable. His suggestions and advice were relevant also for the development of the work presented herein.

APPENDIX: CRITICAL FIELDS NOTATIONS AND NORMALIZATIONS

We briefly review the notations and normalizations of critical fields used in long Josephson junction research. This review can be helpful as different normalizations, notations, and physical unit systems often cause confusion. We will refer to the modulus of fields in the following.

We begin with the Solymar book[15] (SB) (Chap. 12), where SI units are used with the only exception that the unit of the magnetic induction B is expressed in G. We also refer to the modulus of the charge of the Cooper pair as $2e$ and not as q in SB. Equation (12.21) and Fig. (12.5) of SB represent a clear reference for the normalization that we use. In particular, the B field is normalized to $\Phi_0/2\pi d\lambda_j = \mu_0 \lambda_j j_c$. Using this normalization, we see in Fig. 12.5 of SB that the point where the theoretical expression for the first lobe of the Josephson current of a $(10\,\lambda_j)$-long in-line junction extrapolates to zero is 2. It follows trivially that the normalizing H field in SI units would be $\lambda_j j_c$. Note that the lower critical field defined in Eq. (12.39) as $B_{c1} = (4/\pi)\lambda_j j_c$ is not the normalizing factor for all the figures of Chap. 12. This field is the lowest field for which the Meissner solution becomes unstable. The highest field for which the Meissner solution is possible (i.e., our H_0) is defined as $B_x = 2\mu_0 \lambda_j j_c = (\pi/2) B_{c1}$ on p. 197.

The same field normalizing factor used in SB was used in the work of Owen and Scalapino[15] (OS) with the only difference being that cgs units were used. Therefore, the normalizing field of OS is $\Phi_0 c/2\pi d\lambda_j = (4\pi/c)\lambda_j j_c$ and the maximum field for which the Meissner solution is possible is twice this value. Note that in the work by Goldman and

Kreiseman[34] (their paper followed the OS work in the same issue of Phys. Rev.), where the data on the magnetic-field dependence of the currents in long junctions were reported, the field that we have defined as H_0 is called H_{c1}.

Gaussian units were also used by Barone-Paternó (BP),[14] but a factor of 2 is missing in the denominator of the right-hand side of the equation defining H_{c0} on p. 103. However, the definition of the lower critical field H_{c1} on p. 109 is correct. We also note that the field H_0 defined on p. 117 of BP is not the lower critical field, but using the same BP notations $H_0=2H_{c0}=(8\pi/c)\lambda_J J_c$ (we have inserted the correction for H_{c0} written above). Thus, a factor of 2 must multiply the numerator of the right-hand side of the equation defining H_0. With this correction the plots of Figs. 5.17 and 5.10 (in this last figure H_0 must be the normalizing field) of BP are consistent with Vaglio's original paper,[35] with the OS work, and with our notation.

Gaussian units were also used in the paper by Kulik[32] whose definition of the lower critical field is consistent with ours: instead the notation H_s is used for our H_0. We note, however, that in this paper the magnetic penetration is $d=2\lambda_L$ because two identical superconductors are considered. In the recent work of Chen and Hernando[33] instead the same parameter is introduced by setting $2d=2\lambda_L+t$. Thus, these factors of 2 should be taken into account when comparing the critical fields defined in these papers with ours.

A last technical comment concerns the normalizations used in the works of Erné, Ferrigno, and Parmentier (EFP).[26] We can match the normalizations used in these papers to ours simply by dividing their normalized field current ($M=I_F/I_0$) by the number of units occupied by the equivalent of the Josephson penetration depth (which is 10 for the work of Ref. 26). Thus, the EFP value $M=8$, for example, is equivalent to our $\eta=0.8$ and a field value $M=20$ would be the $\eta=2$ maximum field at which the Meissner solution is possible. We recall that in the notation of EFP the quantity indicated as λ_J is not a length but a number. In order to obtain a length one should multiply λ_J for the unit interval sectioning the long junction Δx.

*Present address: Institut für Schicht—und Ionentechnik, Forschungszentrum Jülich GmbH, D-52425 Jülich, Germany.

[1] R. D. Parmentier, in *The New Superconducting Electronics*, edited by H. Weinstock and R. W. Ralston (Kluwer, Dordrecht, 1993), pp. 221–248.

[2] N. Grønbech-Jensen, Phys. Lett. A **169**, 31 (1992); Phys. Rev. B **47**, 5504 (1993); M. Cirillo, G. Rotoli, A. R. Bishop, N. Grønbech-Jensen, and P. S. Lomdahl, *ibid.* **52**, 506 (1995).

[3] M. Cirillo, in *Nonlinear Superconductive Electronics and Josephson Devices*, edited by G. Costabile, S. Pagano, N. F. Pedersen, and M. Russo (Plenum, New York, 1991), pp. 297–306.

[4] T. Holst, J. Bindslev Hansen, N. Grønbech-Jensen, and J. Blackburn, Phys. Rev. B **42**, 127 (1990).

[5] D. W. McLaughlin and A. C. Scott, Phys. Rev. A **18**, 1672 (1978).

[6] V. P. Koshelets, A. V. Shchukin, S. V. Shitov, and L. V. Filippenko, IEEE Trans. Appl. Supercond. **3**, 2524 (1993); Y. M. Zhang and D. Winkler, IEEE Trans. Microwave Theory Tech. **4**, 726 (1994).

[7] T. Nagatsuma, K. Enpuku, F. Irie, and K. Yoshida, J. Appl. Phys. **54**, 3302 (1983).

[8] M. A. H. Nerenberg, P. A. Forsyth, Jr., and J. A. Blackburn, J. Appl. Phys. **47**, 4148 (1976); M. A. H. Nerenberg and J. A. Blackburn, Phys. Rev. B **9**, 3735 (1974).

[9] A. V. Ustinov, J. Mygind, N. F. Pedersen, and V. A. Oboznov, Phys. Rev. B **46**, 578 (1992); A. V. Ustinov, J. Mygind, and V. A. Oboznov, J. Appl. Phys. **72**, 1203 (1992).

[10] M. G. Castellano, G. Torrioli, F. Chiarello, C. Cosmelli, A. Costantini, P. Carelli, G. Rotoli, M. Cirillo, and R. L. Kautz, Phys. Rev. B **54**, 15 417 (1996).

[11] M. Cirillo, F. Santucci, P. Carelli, M. G. Castellano, and R. Leoni, J. Appl. Phys. **73**, 8637 (1993).

[12] S. Pace and U. Gambardella, J. Low Temp. Phys. **62**, 197 (1986); M. Cirillo, U. Gambardella, and S. Pace, Phys. Scr. **38**, 600 (1988).

[13] M. Cirillo, A. M. Cucolo, S. Pace, and B. Savo, J. Low Temp. Phys. **54**, 489 (1984).

[14] A. Barone and G. Paternò, *Physics and Applications of the Josephson Effect* (Wiley, New York, 1982).

[15] C. S. Owen and D. J. Scalapino, Phys. Rev. **164**, 538 (1967); L. Solymar, *Superconductive Tunneling and Applications* (Chapman and Hall, London, 1972), Chap. 12.

[16] J. A. Blackburn, J. D. Leslie, and H. J. Smith, J. Appl. Phys. **42**, 1047 (1971).

[17] R. P. Huebener, in *Advances in Electronics and Electron Physics*, edited by P. W. Hawkes (Academic, New York, 1988), Vol. 70, p.1.; T. Doderer, Int. J. Mod. Phys. B **11**, 1979 (1997).

[18] B. Mayer, T. Doderer, R. P. Huebener, and A. V. Ustinov, Phys. Rev. B **44**, 12 463 (1991); S. G. Lachenmann, T. Doderer, R. P. Huebener, D. Quenter, J. Niemeyer, and R. Pöpel, *ibid.* **48**, 3295 (1993).

[19] I. O. Kulik, Zh. Tekh. Fiz. **37**, 157 (1967) [Sov. Phys. Tech. Phys. **12**, 111 (1967)].

[20] M. Cirillo, N. Grønbech-Jensen, M. R. Samuelsen, M. Salerno, and G. Verona-Rinati (unpublished).

[21] A. M. Cucolo, S. Pace, and R. Vaglio, Phys. Lett. **77A**, 463 (1981).

[22] N. Grønbech-Jensen and M. Cirillo, Phys. Rev. B **50**, 12 851 (1994); N. Grønbech-Jensen, P. S. Lomdahl, and M. Cirillo, *ibid.* **51**, 11 690 (1995).

[23] N. Grønbech-Jensen, J. A. Blackburn, and M. R. Samuelsen, Phys. Rev. B **53**, 12 364 (1996).

[24] O. H. Olsen and M. R. Samuelsen, J. Appl. Phys. **52**, 6247 (1981); B. Dueholm, E. Joergensen, O. A. Levring, J. Mygind, N. F. Pedersen, M. R. Samuelsen, O. H. Olsen, and M. Cirillo, Physica B & C **108B**, 1303 (1981).

[25] M. P. Soerensen, N. Arley, P. L. Christiansen, R. D. Parmentier, and O. Skovgaard, Phys. Rev. Lett. **51**, 19 (1983); G. Filatrella, R. D. Parmentier, S. Pagano, P. L. Christiansen, M. P. Sørensen, and N. Grønbech-Jensen, Phys. Lett. A **172**, 127 (1992).

[26] S. N. Erné, A. Ferrigno, and R. D. Parmentier, Phys. Rev. B **27**, 5440 (1981); IEEE Trans. Magn. **MAG-19**, 1007 (1983).

[27] S. Pagano, B. Ruggiero, and E. Sarnelli, Phys. Rev. B **43**, 5364 (1991).

[28] R. E. Eck, D. J. Scalapino, and B. N. Taylor, Phys. Rev. Lett. **13**, 15 (1964).

[29] H. S. J. Van der Zant, D. Berman, T. Orlando, and K. A. Delin, Phys. Rev. B **49**, 12 945 (1994).

[30] D. Winkler, Y. M. Zhang, P. Å. Nilsson, E. A. Stepantsov, and T. Claeson, Phys. Rev. Lett. **72**, 1260 (1994).
[31] T. Doderer, Y. M. Zhang, D. Winkler, and R. Gross, Phys. Rev. B **52**, 93 (1995).
[32] I. O. Kulik, Sov. Phys. JETP **24**, 1307 (1967).
[33] D. X. Chen and A. Hernando, Phys. Rev. B **49**, 465 (1994).
[34] A. M. Goldman and P. J. Kreisman, Phys. Rev. **164**, 544 (1967).
[35] R. Vaglio, J. Low Temp. Phys. **25**, 299 (1976).